Orientation and Conformation of Methyl Pyruvate on Ni(111)

M. Castonguay, J. -R. Roy, A. Rochefort, and P. H. McBreen*

Contribution from the Département de Chimie, Université Laval, Québec (Québec), Canada G1K7P4, and Centre de Recherche en Calcul Appliqué (CERCA) 5160, Boul. Décarie, Bureau 414, Montréal, (Québec), Canada H3X2H9

Received August 16, 1999

Abstract: The molecular orientation and conformation of methyl pyruvate on Ni(111) was studied in the temperature range 105−220 K. The full monolayer formed at 105 K was found to be almost exclusively in the bidentate *cis*-conformation, with the molecular plane oriented perpendicular to the surface. In contrast, the low coverage layer at 105 K was found to be composed of a mixture of *trans*- and *cis*-methyl pyruvate. However, direct exposure at 200−220 K yielded exclusively *cis*-bidentate adsorption at all coverages. The observation of the preferred *cis*-bidentate species is at odds with the adsorption geometry and conformation usually assumed in rationalizations of the enantioselective hydrogenation of methyl pyruvate on chiral-compound modified platinum metal particle catalysts.

Introduction

Both the orientation and molecular conformation of adsorbed layers are determining factors in a variety of properties including chemical reactivity at surfaces.[1] These properties are particularly important for chemisorbed α-ketoesters, such as ethyl and methyl pyruvate, since they undergo enantioselective hydrogenation on chiral compound-modified oxide-supported platinum metal particle catalysts. The heterogeneous asymmetric hydrogenation of α-ketoesters was first reported by Orito twenty years ago[2] and remains the test case reaction in the field.[3,4] A detailed understanding of the reaction mechanism is necessary, given the increasing demand for optically pure materials and because of the technical advantages of heterogeneous catalysts over their homogeneous counterparts, in terms of handling and separation.[5] Considerable progress has resulted from efforts to achieve higher enantioselective excesses[6] and to extend the range of effective chiral modifiers.[3a] Several recent papers have dealt with attempts to gain a molecular level understanding of the interaction between methyl pyruvate and coadsorbed chiral modifiers. Theoretical and molecular mechanics calculations,[3a,i,7] and experimental results,[8] point toward the formation of adsorbed 1:1 complexes[9] either between the α-ketoester and the protonated modifier[3a,10] or between half-hydrogenated methyl pyruvate and the modifier,[3i] depending on the nature of the solvent.

Although the interaction of cinchonidine with Pt(111) has been studied using LEED and XPS,[3i] this is the first report of a surface spectroscopy investigation of the intrinsic interaction of an α-ketoester with a metal surface. The results presented herein were obtained using mainly reflection−absorption infrared spectroscopy (RAIRS). The RAIRS technique is particularly useful in determining the molecular orientation with respect to the surface plane, and may also provide information on the conformation of adsorbed species.[11] Evidently, the molecular orientation imposed by the chemisorption interaction between the ketoester and the metal needs to be taken into account when

(1) (a) McKendry, R.; Theocliten, M. E.; Rayment, T.; Abell, C. *Nature* **1998**, *391*, 566−568. (b) Lopinski, G. P.; Moffatt, D. J.; Wayner, D. D. M.; Wolkow, R. A. *Nature* **1998**, *392*, 909−911. (c) Fang, H.; Giancarlo, L. C.; Flynn, G. W. *J. Phys. Chem. B* **1998**, *102*, 7311−7315. (d) Pertsin, A. J.; Grunze, M.; Garbuzova, I. A. *J. Phys. Chem. B* **1998**, *102*, 4918−4926. (e) Jung, T. A.; Schitter, R. R.; Gimzewski, J. K. *Nature* **1997**, *386*, 696−698.

(2) Orito, Y.; Imai, S.; Niwa, S. *J. Chem. Soc. Jpn*. **1980**, *4*, 670−672.

(3) (a) Baiker, A. *J. Mol. Catal., A* **1997**, *115*, 473−493. (b) Blaser, H. U.; Jalett, H. P.; Muller, M.; Studer, M. *Catal. Today* **1997**, *37*, 441. (c) Wells, P. B.; Wilkinson, A. G. *Top. Catal.* **1998**, *5*, 39. (d) Hutchings, G. *J. Chem. Commun.* **1999**, 301. (e) Pfaltz, A.; Heinz, T. *Top. Catal*. **1997**, *4*, 229. (f) Baiker, A.; Blaser, H. U. In *Handbook of Hetrogeneous Catalysis*; Ertl, G., Knozinger, H., Weitkamp, J., Eds.; VCH: Weinheim, 1997. (g) Baiker, A. *Curr. Opin. Solid State Mater. Sci.* **1998**, *3*, 86. (h) Augustine, R. L.; Tanidyan, S. K.; Doyle, L. K. *Tetrahedron Asymmmetry* **1995**, *4*, 1803. (i) Simons, K. E.; Meheux, P. A.; Griffiths, S. P.; Sutherland, I. M.; Johnston, P.; Wells, P. B.; Carley, A. F.; Rajumon, M. K.; Roberts, M. W.; Ibbotson, A. *Recl. Trav. Chim. Pays-Bas* **1994**, *113*, 465−474. (j) Blaser, H.-U. *Tetrahedron Asymmetry* **1991**, *2*, 843.

(4) (a) Mallat, T.; Bodnar, Z.; Minder, B.; Borszeky, K.; Baiker, A. *J. Catal*. **1997**, *168*, 183. (b) Burgi, T.; Baiker, A. *J. Am. Chem. Soc*. **1998**, *120*, 12920. (c) Gamez, A.; Kohler, J.; Bradley, J. *Catal. Lett*. **1998**, *55*, 73. (d) Sun, Y.; Landau, R. N.; Wang, J.; LeBlond, C.; Blackmond, D. G. *J. Am. Chem. Soc*. **1996**, *118*, 1348. (e) Margitfalvi, J. L.; Talas, E.; Hegedus, M. *Chem. Commun.* **1999**, 645. (f) Margitfalvi, J. T.; Tfirst, E. *J. Mol. Catal. A Chem.* **1999**, *139*, 81. (g) Sun, Y.; Wang, J.; LeBlond, C.; Landau, R. N.; Laquidara, J.; Sowa, J. R., Jr; Blackmond, D. G. *J. Mol. Catal., A* **1997**, *115*, 495. (h) Augustine R. L.; Tanielyan, S. K. *J. Mol. Catal., A: Chem.* **1997**, *118*, 79. (i) Blaser, H. U.; Garland, M.; Jalett, H. P. *J. Catal.* **1995**, *144*, 569.

(5) Thomas, J. M.; Maschmeyer, T.; Johnson, B. F. G.; Shepard, D. S. *J. Mol. Catal., A: Chem*. **1999**, *141*, 139.

(6) (a) LeBlond, C.; Wang, J.; Andrews, A. T.; Sun, Y.-K. *J. Am. Chem. Soc*. **1999**, 121. (b) Zuo, X.; Liu, H.; Liu, M. *Tetrahedron Lett.* **1998**, *39*, 1941. (c) B. Torok.; Felfoldi, K.; Szakonyi, G.; Balazsik, K.; Bartok, M. *Catal. Lett.* **1998**, *52*, 81. (e) Blaser, H. U.; Jalett, H. P.; Wiehl, J. *J. Mol. Catal.* **1991**, *68*, 215.

(7) (a) Schürch, M.; Heinz, T.; Aeschimann, R.; Mallat, T.; Pfaltz, A.; Baiker, A. *J. Catal.* **1998**, *173*, 187−195. (b) Schwalm, O.; Minder, B.; Weber, J.; Baiker, A. *Catal. Lett.* **1994**, *23*, 271−279. (c) Schwalm, O.; Weber, J.; Minder, B.; Baiker, A. *Int. J. Quantum Chem*. **1994**, *52*, 191−197. (d) Schürch, M.; Schwalm, O.; Mallat, T.; Weber, J.; Baiker, A. *J. Catal.* **1997**, *169*, 275−286. (e) Schwalm, O.; Weber, J.; Minder B.; Baiker, A. *J. Mol. Struct*. **1995**, *330*, 353−357.

(8) (a) Burgi, T.; Zhou, Z.; Kunzle, N.; Mallat, T.; Baiker, A. *J. Catal.* **1999**, *183*, 405. (b) Bartok, M.; Felfoldi, K.; Torok, B.; Bartok, T. *Chem. Commun.* **1998**, 2605.

(9) Margitfalvi, J. F.; Tfirst, E. *J. Mol. Catal., A: Chem.* **1999**, *139*, 81. This paper proposes that the 1:1 complex is formed in the liquid phase.

(10) Blaser, H.-U.; Jalett, H.-P.; Garland, M.; Studer, M.; Thies, H.; Wirth-Tijani, A. *J. Catal.* **1998**, *173*, 282.

(11) (a) Zahidi, E.; Castonguay, M.; McBreen, P. H. *J. Phys. Chem.* **1995**, *92*, 17906−17916. (b) Wang, J.; Castonguay, M.; Roy, J.-R.; Zahidi, E.; McBreen, P. H. *J. Phys. Chem.* **1999**, *103*, 4382−4386.

10.1021/ja992944y CCC: $19.00
Published on Web 01/06/2000

Scheme 1. Illustration of One of the Most Widely Proposed Mechanism for the Enantioselective Hydrogenation of Methyl Pyruvate on Cinchonidine Modified Pt/Al_2O_3

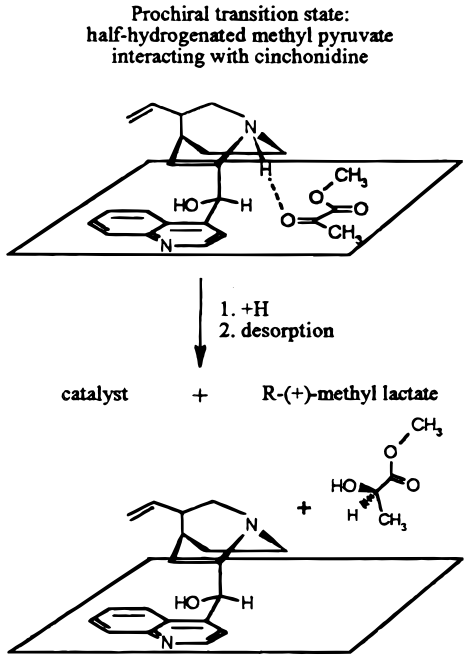

considering possible interactions with the chiral-modifier. The issue of the conformation of adsorbed methyl pyruvate is also of obvious importance in any considerations of the mechanism for the heterogeneous asymmetric hydrogenation reaction. The reaction intermediate proposed frequently in the heterogeneous catalysis literature, and illustrated in Scheme 1, is partly based on the assumption that the molecular plane of the α-ketoester lies parallel to the surface and that the molecule is adsorbed in the *trans*-conformation.[3] However, as pointed out by several authors,[3a,h,i] these assumptions have not been directly verified. In fact, the present study provides evidence contrary to the often proposed conformation and orientation of chemisorbed methyl pyruvate.

Infrared spectra of methyl pyruvate in a variety of nonadsorbed phases were reported by Wilmshurst and Horwood.[12] The crystalline phase was found to be entirely in the planar *trans*-conformation, whereas the planar *cis*-conformation was also present in the glassy, liquid, solution and vapor phases. The *cis*-conformer is the less stable liquid phase conformer by approximately 0.65 kcal/mol, as determined by temperature-dependent IR measurements. Simons et al[3i] estimated the *cis*−*trans* rotational barrier to be 5 kcal/mol on the basis of molecular dynamics calculations. Density functional theory (DFT) calculations presented in this paper place the rotational barrier in isolated methyl pyruvate at less than 3.5 kcal/mol 3.5 kcal/mol. The DFT calculated dipole moments for the *cis* and *trans* conformations are 4.66 and 1.55 D, respectively.

In addition to the possibility of chemisorption-induced conformational change, the interaction of methyl pyruvate with a metal surface is interesting due to the presence of two nonequivalent carbonyl groups: a keto and an ester carbonyl group. Ketone and ester molecules such as acetone and ethyl formate can bond to metal surfaces through a carbonyl lone pair/Lewis acid type interaction.[13,14] Simultaneous lone pair/Lewis acid bonding of both carbonyl groups to the surface would only be possible for methyl pyruvate adsorbed in the *cis*-conformation. Interestingly, chelation of carbonyl compounds to Lewis acid catalysts is a particularly effective approach in homogeneous asymmetric synthesis.[15]

Experimental Section

The experiments were performed on a two-level UHV system equipped with a Mattson Galaxy 4020 FT-IR spectrometer/MCT detector and a quadrupole mass spectrometer on the lower level, and a PHI ESCA spectrometer on the upper level. The base pressure of the chamber was 2×10^{-10} Torr. Both sample cleaning and gas dosing were carried out in the upper level. The Ni(111) monocrystal, purchased from Monocrystals Inc., was cleaned by repeated Ar^+ sputtering, hydrogen treatment, and annealing to 950 K. Surface cleanliness was verified using ESCA spectroscopy until contaminants could no longer be detected. Liquid methyl pyruvate was purified by repeated freeze−thaw cycles in the gas handling line to the vacuum chamber. The final purity was assured by NMR analysis of samples taken from a liquid nitrogen trap in the gas handling line.

The optical path of the IR experiment has been previously described.[14] The setup has a sufficiently high signal-to-noise ratio to provide the possibility of the measurement of time-resolved spectra during gas exposure. The spectra, acquired at a rate of one every 30 s, are expressed in absorbance units and represent the ratio of 100 sample scans to 800 background scans. Thus, for example, up to 25 spectra were recorded during exposure at a background pressure of 1×10^{-8} Torr prior to the emergence of absorption bands characteristic of multilayer methyl pyruvate. The ability to follow the RAIRS signal in such a detailed manner during gas exposure greatly facilitates an overall appreciation of how the spectra change as a function of surface coverage. Many additional experiments were performed at fixed coverages and slower acquisition times in order to confirm which bands were real. The latter measurements also allow us to rule out, or to note, any effects due to the formation of metastable adsorbed states.

The calculations were performed using the deMon-KS[16] software based on the density functional theory-generalized gradient approximation (DFT-GGA) formalism. The NLSD functionals of Becke[17] for exchange and the recent Lap1 scheme[18] for correlation were employed. Double-ξ plus polarization (DZVP) all-electron basis sets were used for the carbon and oxygen atoms, and a double-ξ (DZP) basis set for hydrogen atoms. A model core potential (MCP) that includes corrections for scalar relativistic effects[19] in conjunction with a double-ξ basis set for the valence shell was used for the nickel atom. The contraction pattern for the C and O atoms was (621/41/1*), and (41) for the H atoms. Auxiliary charge density (CD) and exchange-correlation (XC) basis sets are denoted (4,3,4,3) for carbon and oxygen, and (4,4) for hydrogen. An explicit treatment of 3p, 4s, 4p, and 3d orbitals was done for the MCP of Ni (Ni^{+16}) atom. The contraction pattern was (311/31/311) for the Ni atom valence electron orbital basis set, and (3,4,3,4) for the CD and XC basis sets.

The geometries of the complexes were fully optimized by applying the energy gradient expression developed by Fournier.[20] The normal frequencies were determined by diagonalizing the Hessian matrix constructed by numerical differentiation of analytical gradients calcu-

(12) Wimshurst, J. K.; Horwood, J. F. *Aust. J. Chem.* **1971**, *24*, 1183−1191.

(13) Anton, B. A.; Avery, N. R.; Toby, B. H.; Weinberg, W. H. *J. Am. Chem. Soc.* **1986**, *108*, 684−694.

(14) Zahidi, E.; Castonguay, M.; McBreen, P. *J. Am. Chem. Soc.* **1995**, *116*, 5847−5856.

(15) (a) Keck, G. E.; Castellino, S. *J. Am. Chem. Soc.* **1986**, *108*, 3847−3849. (b) Uchiyama, M.; Forumoto, S.; Saito, M.; Kondo, Y.; Sakamoto, T. *J. Am. Chem. Soc.* **1997**, *119*, 11425−11433. (c) Kitamura, M.; Ohkuma, T.; Inoue, S.; Sayo, N.; Kumobayashi, H.; Akutagawa, S.; Ohta, T.; Takaya, H.; Noyori, R. *J. Am. Chem. Soc.* **1988**, *110*, 629−631. (d) Wuest, J. D. *Acc. Chem. Res.* **1999**, *32*, 81.

(16) (a) St-Amant, A.; Salahub, D. R. *Chem. Phys. Lett.* **1990**, *169*, 387. (b) St-Amant, A., Ph.D. Thesis, Université de Montréal, 1992

(17) Becke, A. D. *Phys. Rev. A.* **1988**, *38*, 3098.

(18) Proynov, E. I.; Ruiz, E.; Vela, A.; Salahub, D. R. *Int. J. Quantum Chem. Symp.* **1995**, *29*, 61.

(19) Andzelm, J.; Radzio, E.; Salahub, D. R. *J. Chem. Phys.* **1985**, *83*, 4573.

(20) Fournier, R.; Andzelm, J.; Salahub, D. R. *J. Chem. Phys.* **1989**, *90*, 6371.

Table 1: Infrared Vibrational Frequencies (cm^{-1}) Observed for the Adsorption of Methyl Pyruvate on Ni(111) at Various Coverages, Compared with Values Obtained for the Solution Phase

methyl pyruvate on Ni(111)			solution[a]			
$\theta \approx 0$	$\theta \approx 1$	$\theta > 1$	*cis*	*trans*	mode[a]	description[a,b]
			In Plane Modes (a′ species)			
1740	1685	1755	1762 s	1741 ms	ν_{5-6}	C═O str
1660		1743	1733 ms	1737 vs		
		1680				
1440	1440	1444	1448−1419 ms		ν_{7-9}	CH_3 d
1350		1371	1356 ms			
		1359				
1302	1277	1310	1262 ms	1299 s	ν_{10}	C−O_e str
1275		1278				
		1262				
1188	1188	1196	1213 w	1191 s	ν_{12}	O−CH_3 r
			1108	1056 w	ν_{13}	C−CH_3 r
1000	1014	1004	964 m	1000 s	ν_{14}	C−C str
			Out Of Plane Modes (a″ species)			
			1456−1425 m		ν_{24-25}	CH_3 a, d
1133	1121	1150	1148wm	1133 vs	ν_{26}	O−CH_3 r
		1122				

[a] See refs 12 and 21 for a more detailed attribution. [b] Abbreviations: a: asymmetric; d: deformation; r: rocking; str: stretching

lated at the equilibrium geometry. The displacement of the Cartesian coordinates in the differentiation procedure was 0.05 au. The bond dissociation energies (De) of the complexes were calculated with respect to the ground state species asymptote. Since we focus mainly on the relative stability of the complexes no correction was made for the basis set superposition error (BSSE) in the dissociation energies.

Results

A listing of the medium strong (ms), strong (s), and very strong (vs) solution phase infrared bands observed by Wilmhurst and Horwood[12] are given in Table 1, where they may be compared with band frequencies in the 950−1950 cm^{-1} region for methyl pyruvate on Ni(111). Data for full monolayer, multilayer, and liquid-phase methyl pyruvate, as measured in our laboratory, are displayed in Figure 1. All of the modes labeled strong or very strong in the solution phase spectra are present in the monolayer and submonolayer spectra. The set of bands at approximately 1310 and 1262 cm^{-1} in the liquid-phase and multilayer spectra may be assigned, respectively, to *trans*- and *cis*-methyl pyruvate.[12,21] Appreciable chemisorption-induced shifts in frequency are observed only in the carbonyl stretching region. However, a comparison of the multilayer and chemisorbed layer spectra reveals significant changes in the relative intensities of some bands. In the liquid phase (Figure 1c), multilayer (Figure 1b), and solution-phases (Table 1), the ν(C═O) bands in the 1600−1800 cm^{-1} region and the band at 1133 cm^{-1} are at least as intense as the bands in the 1320−1250 cm^{-1} region. In contrast, the band at 1277 cm^{-1} is the most intense feature in the spectra for monolayer and submonolayer coverages. Contrary to Wilmshurst and Horwood,[12] but on the basis of DFT calculated spectra, we attribute the peak at 1277 cm^{-1} to the C−O_e stretching vibration, where O_e refers to the ester oxygen. This assignment is in line with the usual assignment of an intense band above 1200 cm^{-1} in the IR spectrum of esters. It is also in agreement with the results of a recently published normal coordinate analysis of *trans*-methyl pyruvate.[21] The calculated spectra, and the published normal coordinate analysis, allow us to attribute the 1188 cm^{-1} band to the in-plane OCH_3 rocking mode, and the weak band at 1121 cm^{-1} in the monolayer is attributed to the out-of-plane O−CH_3 rocking mode. Note, however, that the latter mode produces very intense bands at 1135 and 1150 cm^{-1} in the solution-phase and multilayer spectra, respectively.

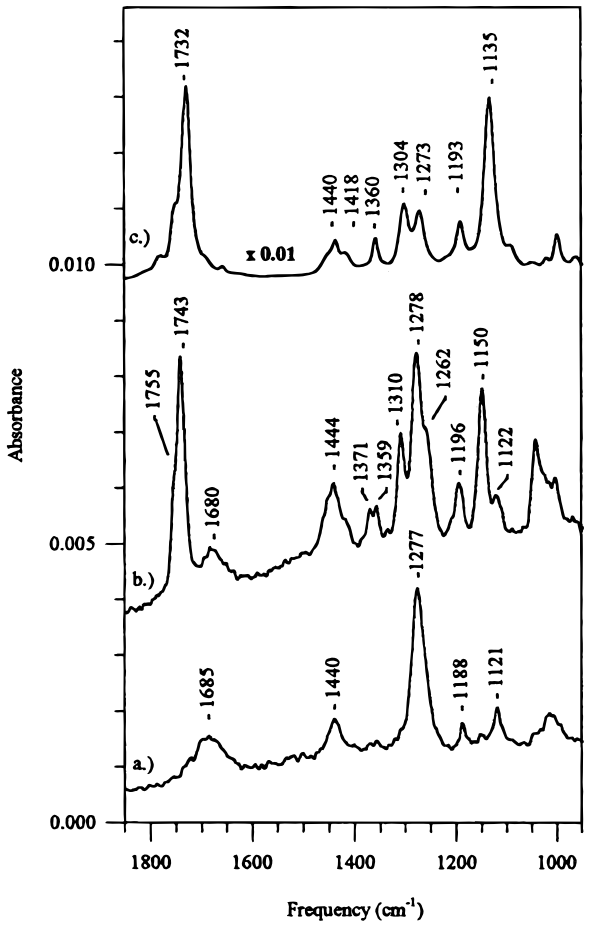

Figure 1. FT-RAIRS spectra for (a) monolayer methyl pyruvate on Ni(111) at 105 K, (b) multilayer methyl pyruvate on Ni(111) at 105 K, and (c) liquid methyl pyruvate.

The spectra displayed in Figure 2 show that the carbonyl stretching region presents a complex set of changes as a function of surface coverage for exposures at 105 K. Three aspects of these variations are immediately evident, and may be described as follows. First, the onset of multilayer formation is clearly demarcated by the emergence of an intense sharp peak at 1743 cm^{-1} with a shoulder to higher frequencies, as seen in Figure 1b. Second, the spectra characteristic of full monolayer coverage (1a and 2f) display a single broad feature in the carbonyl region. As detailed below, the position of this broad band depends sensitively on the dosing temperature. Third, Figure 2 shows that there are bands at 1740 and 1660 cm^{-1} present at low surface coverages. The latter band, in particular, is clearly resolved over a range of coverages. Its contribution decreases as the coverage is increased to the monolayer level. Similarly, a weak band at 1302 cm^{-1} is only clearly resolved at low coverages. The low coverage bands at 1740, 1660, and 1302 cm^{-1} are thus attributed to a single surface species. Figure 3 displays static RAIRS spectra and is included so as to clearly show the differences between approximately half- and full-monolayer spectra for exposure at 105 K. The full coverage spectrum displays a shoulder on the high wavenumber side due to the presence of a small amount of condensed methyl pyruvate, as well as a shoulder at 1652 cm^{-1}. The spectrum taken at half-coverage displays bands at 1652 and 1737 cm^{-1}. The latter band

(21) Dhan, V.; Gupta, R. K. *Ind. J. Pure Appl. Phys.* **1996**, *34*, 830.

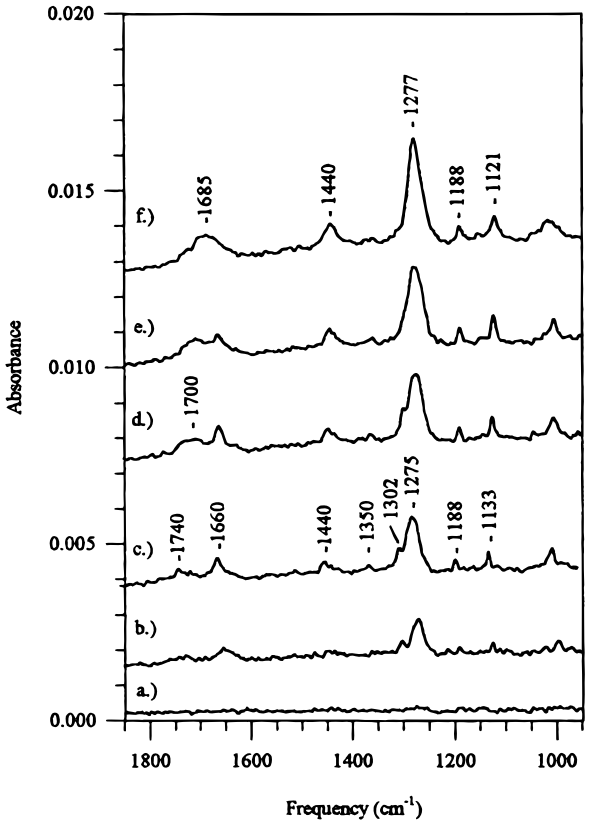

Figure 2. FT-RAIRS spectra recorded during methyl pyruvate exposure to Ni(111) at 105 K. 25 L exposure gives approximately full monolayer coverage. (a) 0 L, (b) 5 L, (c) 10 L, (d) 15 L, (e) 20 L, (f) 25 L.

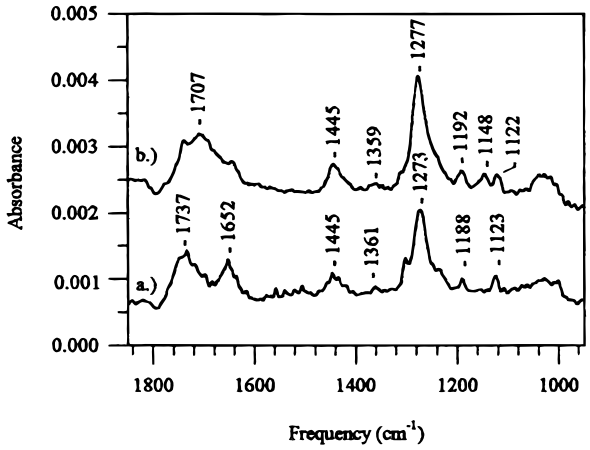

Figure 3. FT-RAIRS spectra of methyl pyruvate recorded in the static mode at 105 K for two exposures: (a) 8 L, (b) 20 L.

shifts down to 1707 cm^{-1} at full coverage. A qualitatively similar red-shift of this band was observed at high coverages for all the exposure conditions used in this study. In contrast, the high-frequency carbonyl band observed at 1740 cm^{-1} at very low coverages (Figure 1) disappears as the coverage is increased.

We show elsewhere that multilayer desorption of methyl pyruvate from Ni(111) occurs at 170 K and that methyl pyruvate dissociates at or above 235 K. The dissociation products in turn yield CO and H_2 peaks in the 360−420 K range accompanied by the deposition of carbon from the equivalent of one methyl group on the surface.[22] The RAIRS spectra displayed in Figure 4 were recorded during exposure at 185 K and therefore display

(22) Castonguay, M.; Roy, J.-R.; McBreen, P. H., manuscript in preparation.

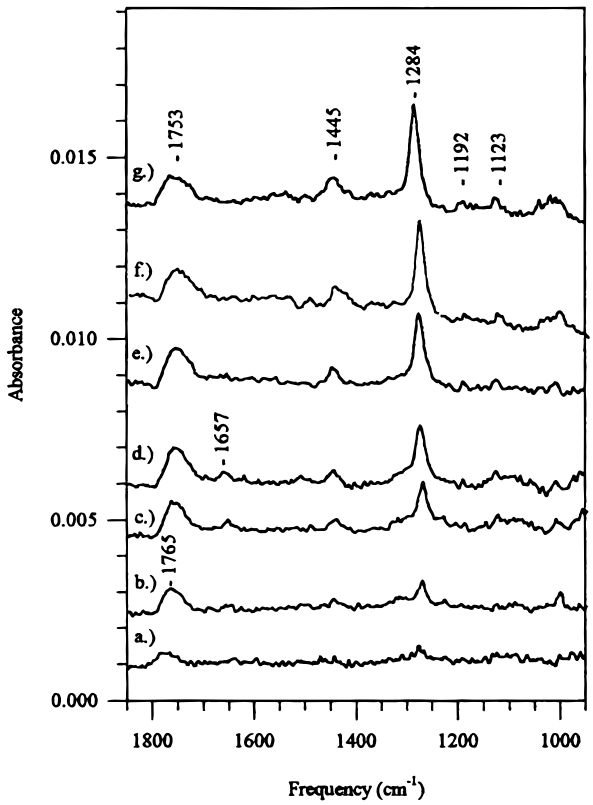

Figure 4. FT-RAIRS spectra of methyl pyruvate adsorbed on Ni(111) at 185 K. (a) 4 L, (b) 12 L, (c) 19 L, (d) 27 L, (e) 34 L, (f) 42 L, (g) 49 L.

no features due to multilayer formation or to surface decomposition species. Exposure at 185 K leads to a single, but broad, carbonyl stretching feature at 1765 cm^{-1} at low coverages shifting to 1753 cm^{-1} at full coverage. The latter frequency is 50−70 cm^{-1} higher than that observed at full monolayer coverage for exposures at 105 K. There is, in addition, a very weak band at 1657 cm^{-1} that initially grows in and then fades out as the monolayer coverage is reached at 185 K. This behavior is similar to that of the more intense 1660 cm^{-1} band observed for adsorption at 105 K. Spectra recorded for exposures at 200−220 K give similar results to those observed at 185 K except that the band in the 1660 cm^{-1} region is absent.

XPS spectra were recorded for the adsorption of methyl pyruvate on Ni(111) at various temperatures between 105 and 200 K. The O(1s) and C(1s) spectra of the multilayer display single peaks at 532.9 and 286.4 eV binding energy, respectively. Sets of O(1s) data as a function of exposure are displayed in Figure 5 for adsorption at 105 and 185 K. Both sets of spectra display a similar double peak structure, particularly at intermediate to monolayer coverages. Saturation exposure at 185 K yields a double-peaked spectrum with maxima at 533.0 and 531.2 eV.

The integrated O(1s) signal is linear as a function of exposure up to saturation of the monolayer at 105 K, Figure 6(a). This direct evidence for a constant sticking coefficient indicates that the surface coverage increases linearly in RAIRS measurements made during gas exposure at 105 K. In contrast, the integrated absorbance data for the carbonyl and $C-O_e$ stretching modes, as shown in Figure 6b and 6c, are not linear in surface coverage. The integrated signal for the envelope of carbonyl stretching bands reaches a maximum at around half-monolayer coverage (or approximately 10 L exposure). A similar, though less pronounced behavior, is seen for the integrated absorbance data

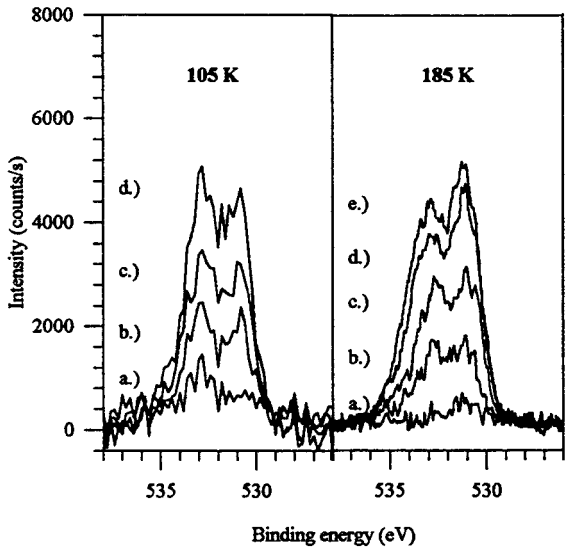

Figure 5. O(1s) spectra as a function of increasing exposure up to approximately monolayer coverage for methyl pyruvate exposure with the Ni(111) sample held at 105 and 185 K.

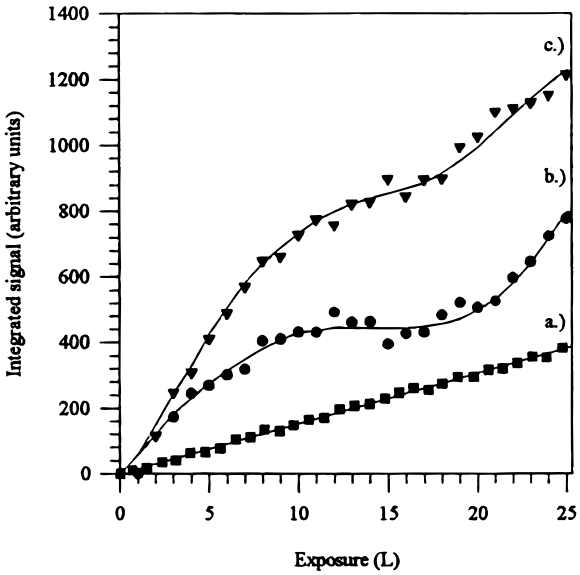

Figure 6. (a) O(1s) integrated XPS signal as a function of exposure of methyl pyruvate at 105 K compared with the integrated absorbance of the (b) C═O and (c) C−O_e infrared bands of methyl pyruvate.

specific to the C−O_e mode. The integrated absorbance of the carbonyl bands increases again as the multilayer is formed. Similar integrated absorbance curves were obtained for methyl pyruvate adsorption at 185 K.

Discussion

Methyl pyruvate displays C_s symmetry and therefore only out-of-plane modes are predicted to be infrared active[23] for the molecule chemisorbed with its molecular plane parallel to a metal surface. Hence, the observation of all of the normally intense in-plane bands indicates that the chemisorbed molecule is not oriented parallel to the surface. On the contrary, the very weak intensity observed for the out-of-plane O−CH_3 rocking mode at 1133 cm^{-1} relative to the C−O_e band at 1277 cm^{-1} suggests that the molecular plane is oriented roughly perpendicular to the surface. The RAIRS activity, albeit weak, of the out-of-plane rocking band nevertheless needs to be accounted for. The possibility that there is a minority nonplanar species on the surface will be discussed below in the context of the *cis*−*trans* rotational barrier.

Scheme 2. Possible Molecular Orientations and Conformations of Methyl Pyruvate on the Ni(111) Surface[a]

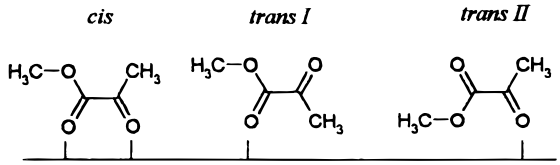

[a] C−C axes of the *trans* I and *trans* II structures are shown parallel to the surface for simplicity. The CH_3 and CH_3O groups may influence this orientation.

A perpendicular orientation with respect to the surface implies that chemisorption occurs via one or both of the carbonyl groups depending on the conformation involved. Equivalently, one could view the geometry of the chemisorbed molecule as resulting from a modification of the conformational equilibrium brought about by the molecule-metal interaction. The most likely adsorption geometry of the *cis*-isomer is with both carbonyls bonded to the metal surface, as illustrated in Scheme 2. This geometry is intuitively favored because it would maximize the adsorption energy by permitting two carbonyl/metal interactions. Such a bidentate interaction would be expected, by reference to data for molecules such as acetone[13] and ethyl formate,[14] to lead to a red-shift of both the keto and ester carbonyl bands. Hence, the broad feature at 1685 cm^{-1} observed at full coverage can be most readily attributed to the two nonresolved carbonyl bands of a bidentate *cis*-configuration. Note that the carbonyl bands in the multilayer (Figure 1(b)) are also not clearly resolved.

In contrast, the adsorption geometry of the *trans*-isomer could be in one of the two configurations (*trans* I and *trans* II) shown in Scheme 2. In both *trans* structures, the Ni−O═C angle is depicted as being close to 120°, as suggested by previous work on the interaction of carbonyl lone pairs with Lewis acids[24,25] and metals.[26] However, steric effects due to the presence of the CH_3 and OCH_3 groups could easily alter this angle.[25] The *trans* I structure involves an ester carbonyl/surface interaction, whereas the *trans* II structure involves a keto carbonyl/surface interaction. Both structures would therefore be expected to yield a clearly resolved set of carbonyl bands, as indicated by the DFT calculated frequencies shown in Scheme 3. Hence, the observation of the set of low coverage peaks, at 1740 and 1660 cm^{-1} is indicative of adsorption in one or other of the *trans* configurations. The band at approximately 1740 cm^{-1} in Figure 2(c) has a vibrational frequency very close to that of liquid *trans*-methyl pyruvate, and this band is therefore attributed to the free carbonyl group in the adsorbed *trans*-conformation. On the other hand, the band at 1660 cm^{-1} clearly has to be attributed, on the basis of literature data for chemisorbed ketones[13] and aldehydes,[27] to a carbonyl group bonded to the surface via a lone pair interaction.

The ν(C−O_e) band and the carbonyl stretching bands are the most sensitive probes of the conformation state of the adsorbed

(23) Greenler, R. G. *J. Chem. Phys.* **1966**, *44*, 310−315.

(24) Shambayati, S.; Crowe, S. W.; Schreiber, S. L. *Angew. Chem., Int. Ed. Engl.* **1990**, *29*, 256−272. (b) Wiberg, K. B.; Marquez, M.; Castejon, H. *J. Org. Chem.* **1995**, *59*, 6817−6822.

(25) LePage, T. J.; Wiberg, K. B. *J. Am. Chem. Soc.* **1988**, *110*, 6642−6650.

(26) Fleck, L. E.; Ying, Z. C.; Feehery, M.; Dai, H. L. *Surf. Sci.* **1995**, *296*, 400−409.

(27) Shekar, R.; Barteau, M. A.; Plank, R. V.; Vohs, J. M., *J. Phys. Chem. B* **1997**, *101*, 7939−7951.

Scheme 3: Density Functional Theory Calculated Vibrational Frequencies for Optimized Geometry Single Nickel Atom Complexes of *trans*-Methyl Pyruvate

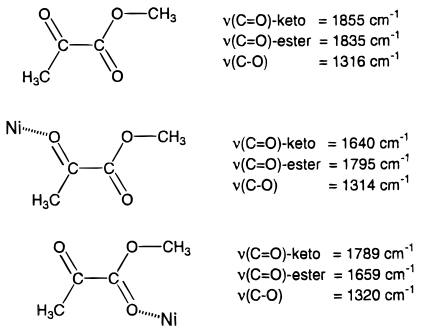

molecule. The evolution of the carbonyl stretching bands confirms the presence of a changing *cis*/*trans* ratio as the surface coverage is increased at 105 K from zero to full monolayer coverage. The band at 1660 cm^{-1} initially increases in intensity with increasing coverage but is dominated by a broad *cis*-conformation peak, at 1685 cm^{-1}, at full coverage. The $\nu(C-O_e)$ band has a clearly resolved shoulder at 1302 cm^{-1} at low coverages. The fact that the shoulder displays the same coverage dependence as the set of *trans*-conformation carbonyl bands favors its attribution to the $\nu(C-O_e)$ mode of adsorbed *trans*-methyl pyruvate. The intense band at 1277 cm^{-1} which is present at all coverages, is then attributed to adsorbed *cis*-methyl pyruvate. The fact that the integrated absorbance is linear in coverage in the zero to half-monolayer region shows that the *cis*-state is present even at the lowest coverages. This conclusion is supported by RAIRS data for *cis*-2,3-butanedione on Ni(111) in that the latter system displays broad and difficult to detect carbonyl bands.[28] The monolayer composition, which is very close to pure *cis*-adsorbed methyl pyruvate, is in stark contrast to that for crystalline methyl pyruvate, where all molecules are in the lower energy *trans* conformation, as well as that for liquid methyl pyruvate, where there is a mixture of *cis* and *trans* conformers.

The band at 1277 cm^{-1}, attributed to the $C-O_e$ stretching band of *cis*-bidentate methyl pyruvate, is only slightly blue-shifted ($\Delta\nu = 15$ cm^{-1}) with respect to the solution $C-O_e$ stretch. In fact, it is not shifted at all with respect to liquid-phase data.[12] In contrast, we have previously shown that the $C-O_e$ stretching frequency of methyl formate, ethyl formate and methyl acetate adsorbed on Ni(111) via the carbonyl group is blue-shifted by up to 80 cm^{-1} with respect to the free molecule.[11] A similar effect is observed for Lewis-acid complexes of many esters.[29] The absence of a shift could be taken to indicate that there is either no, or a very weak, interaction between the ester carbonyl and the surface. However, density functional calculations (Scheme 3) on single nickel atom complexes of *trans*-methyl pyruvate predict almost no shift in the $C-O_e$ stretching frequency even when the nickel is bonded to the ester carbonyl. Similarly no shift is observed in RAIRS studies of *tert*-butyl formate on Ni(111),[30] presumably due to the inductive effect of the *tert*-butyl group. The DFT calculations predict, however, that a keto carbonyl bonded configuration is more stable by 3.5 kcal/mol than the ester-carbonyl bonded configuration. This is in keeping with the accepted relative reactivity of keto- and ester carbonyl groups. By analogy, the keto carbonyl−nickel interaction is expected to be the dominant molecule-surface interaction in the case of bidentate *cis*-adsorbed methyl pyruvate.

The frequency of the *cis*-methyl pyruvate carbonyl band is sensitive to the dosing conditions. Frequencies in the 1765−1750 cm^{-1} region, as observed for adsorption with the sample held in the 180−220 K temperature range, are blue-shifted by 50−80 cm^{-1} with respect to those observed for exposures at 105 K. However, the similarity of the O(1s) spectra in Figure 5, and the qualitative similarity of the RAIRS spectra, for full coverage following adsorption at 105 and 185 K suggests that that the adsorbed species are the same in both cases. Hence, the difference in the carbonyl stretching frequency is attributed to changes in the order of the adlayer. This interpretation is supported by the fact that the broad *cis*-bidentate carbonyl peak appears at progressively higher frequencies in going from spectra recorded during exposure at 105 K (Figure 2), to spectra acquired in the static mode at 105 K (Figure 3), to spectra taken on exposure at 185−220 K. These dosing conditions should lead to progressively more equilibrated layers. Furthermore, the carbonyl stretching frequency value of 1760 cm^{-1} observed for exposure at 200 K is the same as that for solution-phase *cis*-methyl pyruvate (Table 1). Since bidentate chemisorption should lead to a red-shift of the carbonyl band, the chemical shift must be balanced by a blue-shift due to dipole−dipole interactions in the ordered layer. The integrated absorbance plots displayed in Figure 6 are clearly consistent with dipole−dipole coupling.[31] The relatively high observed stretching frequency may also be partly due to intensity borrowing from the keto carbonyl to the higher frequency ester carbonyl band.[31]

The out-of-plane $O-CH_3$ rocking mode observed at 1121 cm^{-1}, although weak in all cases, is most clearly visible for measurements carried out during exposure at 105 K. This suggests that it is characteristic of a poorly ordered layer. The activity of the out-of-plane mode suggests a tilt in some methyl pyruvate species with respect to the plane normal to the surface. One possibility is that the adsorbed *trans*-conformer is present in a nonplanar form, with the molecule bound to the surface via the keto carbonyl and with the ester moiety ($COOCH_3$) oriented roughly parallel to the surface. DFT calculations predict an upper limit of 3.5 kcal/mol for the rotational barrier of free methyl pyruvate. The ester moiety is almost equivalent to methyl formate, and the condensation energy for methyl formate on Ni(111) is approximately 7 kcal/mol, at least twice the rotational barrier. RAIRS data for 2,3-butadione on Ni(111) clearly show that chemisorption induced *trans*−*cis* isomerization takes place[28] despite a rotational barrier of 7−8 kcal/mol for the free molecule.[32] Hence the proposed nonplanar species is plausible. Such a nonplanar species might explain why the $C-O_e$ band at 1302 cm^{-1} and the free carbonyl band attributed to *trans*-methyl pyruvate are so weak. However, it must be emphasized that the *trans*-conformer is not observed for exposures at 200 K, and it is almost absent at full coverage for exposure at 105 K. Hence, the *cis*-conformer is the important stable molecular species on the Ni(111) surface.

The observed orientation and conformation of methyl pyruvate on Ni(111) is in opposition to what is usually assumed when considering its asymmetric hydrogenation on cinchonidine-modified platinum. For example, it is typically assumed that methyl pyruvate adsorbs, by analogy with buta-1,3-diene,[3] with its molecular plane parallel to the surface (as in Scheme

(28) Roy, J.-R.; Castonguay, M.; Rochefort, A.; McBreen, P. H., manuscript in preparation.
(29) Taliander, M.; Liguier, J.; Taillandier, E. *J. Mol. Struct.* **1968**, *2*, 437.
(30) Castonguay, M.; Roy, J.-R.; McBreen, P. H., manuscript in preparation.
(31) Person, B. N. J.; Ryberg, R. *Phys. Rev. B* **1981**, *24*, 6954.
(32) Allinger, N. L.; Fan, Y. *J. Comput. Chem.* **1995**, *15*, 251.

1). However, buta-1,3-diene differs from methyl pyruvate in that the former is a truly planar molecule, whereas the methyl group hydrogens of methyl pyruvate protrude from the molecular plane. Hence, a flat-lying geometry for methyl pyruvate would be difficult to justify on the basis of the detailed insights on the chemisorption of carbonyl molecules given by the theoretical work of Sautet et al.[33] Furthermore, it may also be an error to restrict consideration to *trans*-methyl pyruvate, despite the fact that the *cis*-conformation does not figure in any of the mechanisms proposed to date for the heterogeneous enantioselective hydrogenation of α-ketoesters. The present results show that the *cis*-conformation is the more stable adsorbed structure on Ni(111). In fact, one could speculate that the ester carbonyl−metal interaction in *cis*-bidentate methyl pyruvate plays a role in anchoring the molecule to the surface at some points along the reaction coordinate leading to enantioselective OH and CH bond formation at the keto carbonyl function.

Conclusions

The adsorption geometry adopted by methyl pyruvate on Ni(111) is quite distinct from that proposed in reaction schemes for its enantioselective hydrogenation on alkaloid modified platinum. In particular, the present results show that although *trans*-methyl pyruvate is the more stable isomer in the gas, liquid, and solid phases, the presence of bidentate *cis*-adsorbed methyl pyruvate should be considered in mechanisms for the enantioselective hydrogenation reaction. Furthermore, it should be assumed that the *cis*-bidentate species is oriented perpendicular to the surface. Molecular modeling results in the catalysis literature clearly point toward an adsorbed 1:1 complex between the α-ketoester and the chiral modifier. The present spectroscopic data suggest that the specific nature of the pyruvate metal interaction also needs to be taken into account. Whether the spectroscopically observed *cis*-bidentate species is kinetically significant is a much more complex question.

Acknowledgment. We gratefully acknowledge financial assistance from NSERC (Operating Grant) and FCAR (Équipe et Centre de Recherche (CERPIC)). M.C. acknowledges the receipt of an NSERC graduate scholarship. The machining and electronics support of André Bouffard, Réjean Drolet and Jean Laferrière are gratefully acknowledged.

JA992944Y

(33) Delbecq, F.; Sautet, P. *Surf. Sci.* **1993**, *295*, 353−373.